Int. J. Nanosci. Nanotechnol., Vol. 18, No. 2, June 2022, pp. 123-133

Preparation of Composites of Antibacterial Materials Based on Bacterial Cellulose and Silver Nanoparticles for Wound Healing

Bibigul Rakhimova[1,2], Kenes Kudaibergenov[1], Larissa Sassykova[1,*], Galiya Spanova[1], Sestager Aknazarov[1,2] and Marat Tulepov[1]

[1]Faculty of Chemistry and Chemical Technology, Al-Farabi Kazakh National University, 050040, Almaty, Kazakhstan
[2]Scientific and Production Technical Center "Zhalyn" LLP, 050012, Almaty, Kazakhstan

(*) Corresponding author: larissa.rav@mail.ru
(Received: 26 June 2021 and Accepted: 8 January 2022)

Abstract

This study examined the preparation of composites of Bacterial Cellulose (BC) / silver nanoparticles (Ag NPs) using a substrate for the fermentation of the bacteria Gluconacetobacter xylinus C-3 and a reducing agent for the synthesis of silver nanoparticles in situ. The presence of silver in the BC/ Ag NPs composites was confirmed by various characterization tests. Thus, according to Scanning Electron Microscopy, the average size of silver was recorded at 700 nm. X-ray phase analysis showed an increase in the size of cellulose crystallites up to 122 Å with a decrease in the amount of silver nanoparticles. According to UV-visible spectroscopy, an identification peak was found between 420-580 nm. Measurements of the percentage of water absorption and the edge angles of wetting with water confirmed the structures of the resulting nanocomposites - with a smaller pore diameter and a narrow pore distribution over the film size, depending on the silver content. Using the disk diffusion method, excellent antimicrobial activity was shown with a decrease in the number of bacteria in relation to the pathogenic microorganism Staphylococcus (S.) aureus, Pseudomonas (P.) aeruginosa, Escherichia (E.) coli.

Keywords: *Antimicrobial activity, Bacterial cellulose, Composites, Hydrothermal synthesis, Silver nanoparticles, Turkevich citrate method.*

1. INRODUCTION

Recently, biodegradable materials, biocompatible with body tissues, based on Bacterial Cellulose (BC) for the treatment of skin diseases, burns and wounds of various etiologies, have attracted great interest [1]. BC is known for its many desirable properties such as stability, biocompatibility, extensive chemical modification, biodegradability, and large surface area. Although BC and plant-derived cellulose have the same chemical structure of the linear chains of β-1,4-glucan, there are still many differences in their physical properties [2-5].

BC is produced by various strains of acetic acid bacteria (for example, *Gluconacetobacter xylinus*, formerly known as *Acetobacter xylinum*) and is also suitable as a drug delivery system and wound dressing. The BC produced by *Gluconacetobacter xylinus* is markedly different from the cellulose obtained from trees and cotton, which does not contain lignin and hemicellulose.

However, bacterial cellulose, a bio-polymer synthesized by the bacteria *Gluconacetobacter xylinus*, has a unique nanostructure, but does not have an antimicrobial effect [6]. The antimicrobial activity of wound dressings plays an important role in fighting infections and promotes wound healing during their treatment.

In order to give BC antimicrobial properties, many studies have prepared composite materials based on BC with an

antibacterial function as a dressing material for wounds [7]. To prepare BC-based composites with good antibacterial properties as wound dressings, three methods can be used: adding antibiotics, combining with inorganic antibacterial agents, and combining with organic antibacterial agents. The addition of antibiotics is the most commonly used method that has become widespread in clinical practice. Inorganic antibacterial agents have excellent antibacterial properties and have great prospects for application in the field of biomedicine [8-20]. Natural organic antibacterial substances have attracted wide attention due to their good biocompatibility and biodegradability [8]. In ref. [12] the authors analyzed the chemical composition of *Atlantic pistachio* fruit oil and studied the wound healing and anti-inflammatory effects of bacterial cellulose absorbed by the oil on an in vivo model of a burn wound.

Histological analysis showed that fruit oil-coated bacterial cellulose significantly reduced the number of neutrophils as an indicator of inflammation compared to negative control or positive control ($p < 0.05$). Wound closure was faster in the fruit oil-coated bacterial cellulose group compared to other treatments ($p < 0.05$).

Chemical modification is used to give bacterial cellulose additional adsorption properties and antimicrobial activity. The combination of inorganic antibacterial agents and BC has always been a hot spot of research, especially nano-antibacterial materials consisting of metals / metal oxides and BC. Immersion, reduction, and deposition are commonly used composite methods, and the choice of composite methods depends on different situations [13].

Silver nanoparticles (Ag NPs) have attracted a lot of attention due to their broad-spectrum antibacterial properties. A large number of studies have shown that these nanoparticles can kill bacteria, but the antibacterial mechanism of Ag NPs is still not clear. Some researchers believe that when the silver ion (Ag^+) released from Ag NPs reaches a certain concentration range, it inhibits bacterial growth, destroys the cell membrane, and prevents DNA replication and transcription. In addition, silver or silver ions can promote the production of intracellular active forms of the cell, thereby destroying the structure and function of bacterial cells [14-17]. BC can be combined with Ag NPs in various ways to produce BC-based antibacterial materials. The aldehyde or carboxyl groups of BC are usually prepared by oxidation with oxidizing agents such as sodium periodate and 2,2,6,6-tetramethylpiperidinyloxy (TEMPO).

Sodium periodate can selectively oxidize hydroxyl groups at the C_6 BC position to form an aldehyde group. Due to the use of more sodium periodate and a longer oxidation time, it is possible to obtain oxidized nanocellulose with a higher content of aldehyde groups. TEMPO can bind on the surface of nanocellulose under aqueous conditions and convert the hydroxyl group at the C_6 position into aldehyde or carboxyl functional groups [18, 19]. Various methods for the preparation of BC composites with Ag NPs have been developed and their pronounced antibacterial activity has been shown [20].

The aim of the work was to study the physico-chemical and antibacterial properties of nanocomposites of BC (bacterial cellulose) with Ag NPs (silver nanoparticles).

2. MATERIALS AND METHODS

2.1. Bacterial Cellulose Films

Bacterial celluloses were synthesized in the culture of acetic acid bacteria *Gluconacetobacter xylinus C-3* and the culture medium *Hestrina-Shramma*. The optimized growth environment and cultivation conditions ensure high BC yields in surface static culture. To obtain a purified BC film, it was separated from the culture liquid, and to remove bacterial cell

residues and components, the culture medium was immersed in 0.1% NaOH solution and treated for 30 minutes at a temperature of 80-100ºC, followed by washing with distilled water to pH 7.

2.2. Preparation of Ag NPs and Composites of BC/Ag NPs

Two methods were used to obtain BC composites with Ag NPs. First, a previously developed method for producing colloidal silver nanoparticles by the Turkevich citrate method was used for the synthesis of nanosilver [21], and the temperature regime for boiling $AgNO_3$ (200°C) and the mixing speed on a magnetic stirrer (350 rpm) were used. The hydrothermal method was also used: without the use of any catalysts, using the disks of the BC layer as a reducing agent and stabilizer.

A solution of 25 ml of $1x10^{-3}$ mol/L $AgNO_3$ prepared in distilled water was brought to a boil, after which $1x10^{-2}$ mol/L $Na_3C_6H_5O_7$ was added drop by drop and a change in the color of the solution to light yellow was observed. The change in the color of the solution changed from colorless to light yellow, which indicated the reduction of silver ions.

Heating was continued for 15 minutes, and then the solution was cooled to room temperature for use as a filler for the preparation of BC / Ag NPs. The cleaned wet films of BC were cut into discs with an average diameter of 3 cm, then placed in a flask with a 0.001 M solution of Ag NPs and heated for 60 minutes to 30°C, 60°C, and 90 °C.

Also, the effect of various concentrations of $AgNO_3$ in the reaction medium was estimated for 0.01M, 0.001M and 0.0001M, at a temperature in the system of 60°C. After that, the samples were washed several times with a 30% ethanol solution. Silver-containing BC films were dried at 60°C to constant weight.

2.3. Characteristics Determination

2. 3.1. Scanning Electron Microscopy

The structure of samples of BC films with Ag NPs was studied on a Scanning Electron Microscope (SEM) equipped with the X-ray Spectral Analysis System Quanta 3D 200i Dual system, FEI (USA) in the DGP "National Open-Type Nanotechnology Laboratory" of the al-Farabi Kazakh National University.

2. 3.2. UV-Visible

Absorption spectra of UV-V were obtained using a Varian Cary 500 Scanning Spectrometer. Films of pure and dry cellulose were used as reference materials in a suitable substrate for solid samples.

2.3.3. Water Content Analysis

To determine the water absorption, BC films and BC/ Ag NPs dried to a constant weight were cut into disks with a diameter of 3 cm and immersed in distilled water until the swollen state was reached. Next, the weight change was measured at different times and dried at a temperature of 25°C. This was also done for all types of modified BC films. The water content can be calculated using the following equation:

$$W = \frac{W_b - W_k}{W_k} \quad (1)$$

where: W_b is the mass of the sample with the water content.

W_k is the initial mass of the dried sample.

2.3.4. Wetting Angle

The properties of the surface of the BC membranes were studied using a device for measuring the wetting edge angle-DSA-25E (Kruss, Germany) for measuring the contact edge angles of water droplets by measuring the free surface energy (FSE), followed by data processing using the DSA-4 program.

2.3.5. X-ray Diffractogram of BC and Composites of BC / Ag NPs

X-ray images of the samples were obtained on a DRON-4 diffractometer in

digital form using copper radiation. The sample shooting mode is as follows: the voltage on the X-ray tube is 35 kV, the tube current is 20 mA, the goniometer movement step is 0.05º 2θ and the intensity measurement time at the point is 1.5 seconds. During the survey, the sample rotated in its own plane at a speed of 60 rpm. The phase analysis was performed using the PCPDFWIN and Search Match software with the PDF-2 diffractometric database. The measurement results were digitally processed in the ORIGIN program.

2.3.6. Antimicrobial Susceptibility Test

The antimicrobial susceptibility test for the BC /Ag NPs composites was studied in cultures of reference strains of pathogenic microorganisms: *Escherichia (E.) coli* ATCC 25922, *Pseudomonas (P.) eruginosa* ATCC 27853, as models of gram-negative bacteria, and *Staphylococcus (S.) aureus* ATCC 25923, as a model for gram-positive bacteria.

Microorganisms were cultured in tubes containing 3 ml of sterile infusion of the brain heart (IBH) and incubated at 37°C per day. Sufficient inoculum was added to new tubes at 0.5 McFarland density (~ 108 CFU / ml). Antimicrobial activity was assessed by method of disk diffusion in MX agar plates. About 15-20 ml of MX agar was poured into sterile Petri dishes, after it solidified, a new bacterial seed material was evenly distributed on the lawn surface with a sterile microbiological loop. The composite sample of BC /Ag NPs was cut into disks with a diameter of 1 cm and sterilized by UV radiation for 2 hours. After sterilization, the discs were placed on the bacterial culture of the Petri dish and placed upside down in the thermostat, then incubated at 35°C for 24 hours.

3. RESULTS AND DISCUSSIONS

The mechanism of interaction of BC with silver ions in the presence of reducing agents is the reduction of Ag^+ ions located both on the surface of microfibrils and intercalated in the cellulose matrix.

Using the Turkevich method, it was possible to obtain Ag NPs with a diameter of aggregates of different shapes in the range from 60 to 200 nm. Despite a number of disadvantages, the citrate method is widely used for the synthesis of Ag NPs due to its simplicity. The citrate ion obtained by dissolving the three-substituted sodium salt of citric acid $C_6H_5O_7Na_3$ in water plays the role of not only a reducing agent, but also a stabilizer of the resulting nanoparticles of zero-valent silver. When the solution is heated and the citrate ion is oxidized, acetondicarboxylic and itaconic acids are formed. These acids are adsorbed on the surface of the particles and control their growth.

Currently, there are two mechanisms that explain the formation and growth of silver nanoparticles as shown in Figure 1.

The reducing and stabilizing effects of the hydroxyl groups of BC act as centers of adsorption, nucleation, and growth of silver nanoparticles.

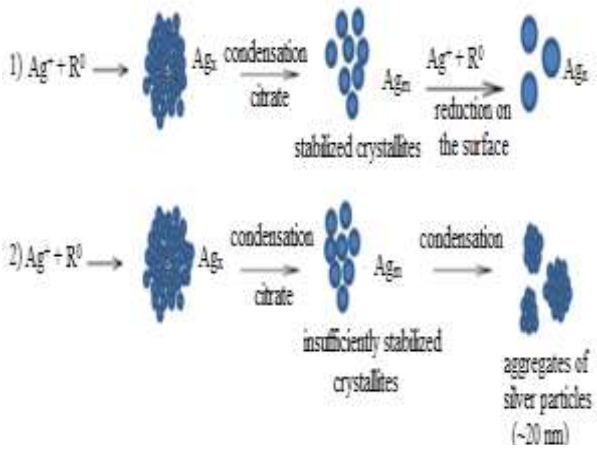

Figure 1. *Mechanisms of growth of Ag NPs stabilized by the citrate anion.*

During the synthesis reaction in an acidic medium, the bacterial cellulose chains break down into small chains with hydroxyl groups (Figure 2).

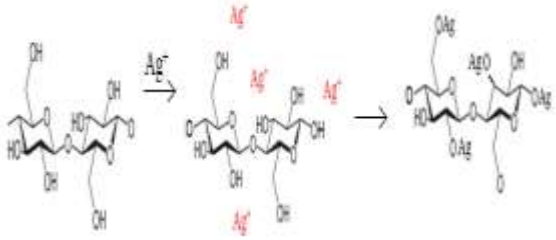

Figure 2. *The role of BC hydroxyl groups in the synthesis of Ag NPs.*

The hydrogen atom is displaced from the hydroxyl group, and the silver ion replaces the hydrogen [21].

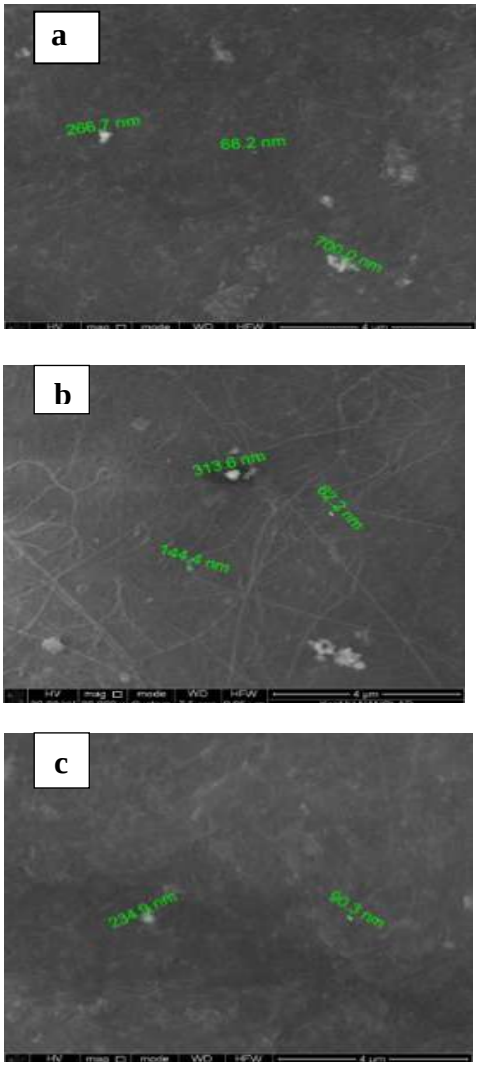

Figure 3. *SEM images of the surface morphology of composite films BC /Ag NPs obtained at different temperatures dried at 40ºC: BC /Ag NPs 30℃ (a), BC /Ag NPs 60℃ (b) and BC /Ag NPs 90℃ (c).*

3.1. Surface Morphology

The morphology of composite films of BC with Ag NPs studied in SEM with an energy-dispersive X-ray Spectral Analysis System, is shown in Figures 3, 4.

A change in the temperature of the medium with a concentration of 0.001 M of Ag NPs affected the size of the silver nanoparticles formed on the surface of the BC films.

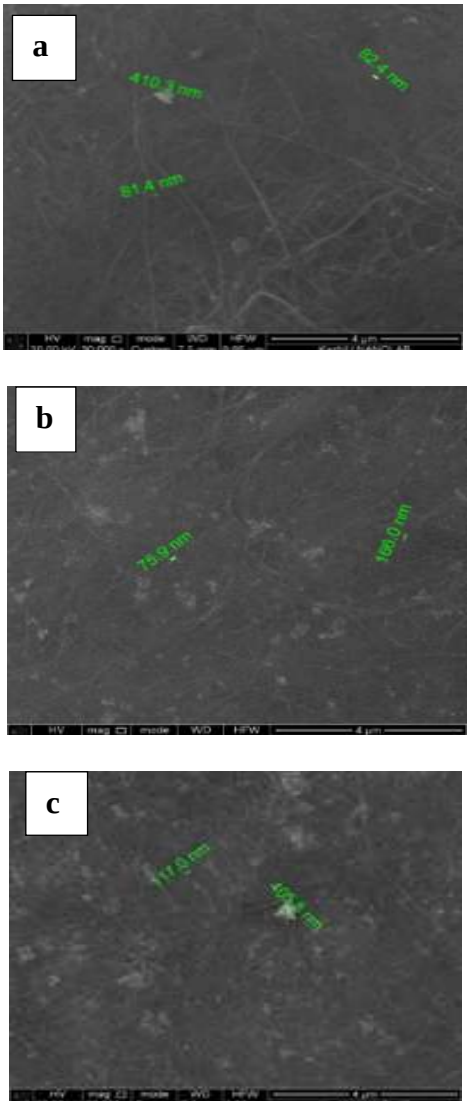

Figure 4. *SEM images of the surface morphology of composite films of BC / Ag NPs obtained at different concentrations of $AgNO_3$ in the medium, dried at 40℃: BC /$AgNO_3$ (0.0001 M) (a), BC /$AgNO_3$ (0.001 M) (b) and BC /$AgNO_3$ (0.01 M) (c).*

In a solution with a concentration of 0.001 M of Ag NPs at 30°C, the

aggregation of the formed silver particles apparently occurred, and their average size was 700 nm.

When the temperature in the reaction solution is increased to 60°C and 90°C, the particle size is significantly reduced to 313 and 234 nm, respectively. In a solution of $AgNO_3$ with different concentrations (0.0001, 0.001 and 0.01 M) with a stable medium temperature at 60°C the sizes of Ag NPs with an average size of 410 nm, 400 nm and 405 nm, respectively, are established.

The average molar percentages of Ag NPs in composite samples slightly depend on the temperature in the system and are 2.81, 3.54, and 3.87 at 30°C, 60°C, and 90 °C, respectively (Table 1). An increase in the concentration of $AgNO_3$ in the reaction solution from 0.0001 M to 0.01 M was accompanied by an increase in the silver content in the composites from 1.17%, 3.78% and 6.12%.

Table 1. *Effect of synthesis conditions on the elemental composition of composite films BC/Ag NPs.*

Average atomic number	Samples						
	BC	Effect of temperature at BC/Ag^0 0.001 M			Effect of $BC/AgNO_3$ concentration at 60°C		
		30 °C	60 °C	90 °C	0.0001 M	0.001 M	0.01 M
C	44.2	42.7	41.5	42.3	42.7	41.5	40.3
O	55.7	53.4	49.8	52.3	52.1	53.7	51.1
N	-	0.6	0.4	0.8	1.3	0.7	1.1
Ag	-	2.8	3.5	3.9	1.2	3.8	6.1

3.2. UV visible

The method of visual observation of the system gives general regularities of the relative sedimentation stability of the studied dispersion and the change in the color of the system in it. For example, for Ag NPs, the color of the systems changes from yellow to black. These methods include optical spectroscopy based on the measurement of the absorption spectrum (Figures 5, 6). By evaluating the absorption spectra, one can observe the recrystallization of Ag NPs with the appearance of an additional absorption band in the dependence of the optical density on the wavelength or a new maximum in the long-wavelength part of the spectrum.

A wide range of silver sols in the initial concentration range of 0.0001 to 0.01 M to produce composite films of BC with Ag NPs was synthesized.

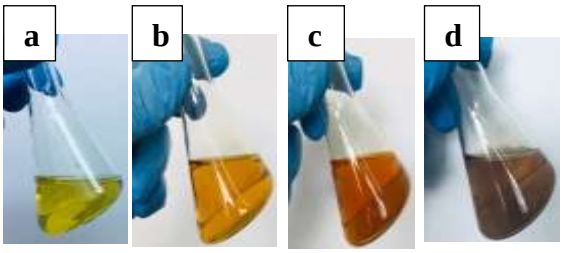

Figure 5*. Optical properties of colloidal Ag NPs using UV-visible absorption spectroscopy. Photos of colloids (A): (a) yellow, (b) light orange, (c) orange and (d) dark orange.*

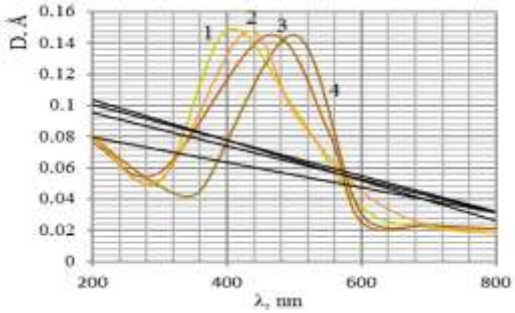

Figure 6. *The UV-visible absorption spectra of Ag NPs colloids at (b) shows the peak wavelength with the full width at half the maximum at (1) 400 nm (64 nm); (2) 427 nm (69 nm); (3) 460 nm (192 nm); (4) 500 nm (160 nm). (1) BC/Ag NPs 60°C, (2) BC/ $AgNO_3$ 0.0001 M, (3) BC / $AgNO_3$ 0.001 M and (4) BC / $AgNO_3$ 0.01 M.*

Spectrophotometric analysis of the samples selected during the synthesis of Ag NPs showed that in the absorption band between 400-600 nm, the presence of metallic Ag NPs in the solution can be observed. In this case, the average size of the Ag NPs obtained is 45-50 nm, as mentioned in the literature [22].

An increase in the absorption intensity at the band maximum is associated with the continuation of the silver reduction process and an increase in the number of particles.

When studying the UV-visible spectrum of the initial BC and the resulting composite films of BC with Ag NPs, a peak was found between 420-580 nm. Thus, the data of the absorption spectrum of the colloidal silver solution (Figure 5,6) indicate the success of the process of obtaining the composite (Figure 7-9).

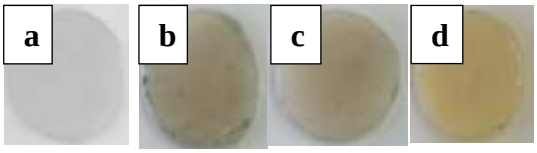

Figure 7. *Photos of raw BC films and BC/ Ag NPs synthesized under three temperature conditions: BC (a), BC/Ag NPs 30°C (b), BC/Ag NPs 60°C (c) and BC/Ag NPs 90°C (d).*

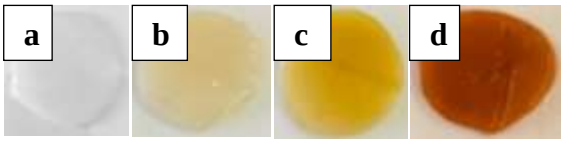

Figure 8. *Photos of raw BC films and BC/ Ag NPs synthesized with different concentrations of $AgNO_3$ in the reaction solution: BC (a), BC / $AgNO_3$ 0.0001 M (b), BC / $AgNO_3$ 0.001 M (c) and BC / $AgNO_3$ 0.01 M (d).*

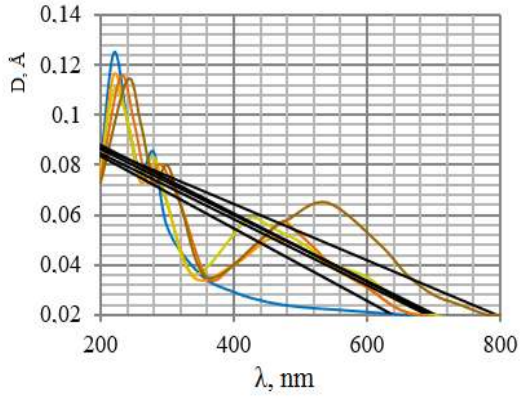

Figure 9. *UV-visible spectra of BC / Ag NPs:●BC;●BC/AgNPs, 60°C;●BC/ $AgNO_3$, 0.0001M;● BC / $AgNO_3$, 0.001 M;●BC/ $AgNO_3$, 0.01 M.*

A change in the temperature of the medium with a solution concentration of 0.001 M Ag NPs had an insignificant effect on the BC structures. Therefore, for comparison, the absorption spectrum of the UV-visible range was obtained for a sample at 60 °C.

The original BC has peaks between 200 and 300 nm, this is due to the bacteria used to make the BC. According to the literature [23], most proteins exhibit optical density in the range of 200–300 nm. The use of $AgNO_3$ solutions of different concentrations (0.0001, 0.001 and 0.01 M) with stabilization of the medium temperature at 60°C provided an absorption spectrum of the UV-visible range between 420-570 nm, respectively.

However, with an increase in the $AgNO_3$ concentration, the absorption intensity at the maximum of the band increases, and this indicates an increase in the silver content in the composite samples.

3.3. Water Absorption Capacity

BC has unique absorption properties - water absorption capacity arising from the three-dimensional structure of nanofibers and high porosity. The composite films of BC gel / Ag NPs obtained in this work had a water - holding capacity under physicochemical conditions, but drying at room temperature led to a significant decrease in its absorption capacity. This may be due to a significant change in the internal structure of the polymer matrix due to the numerous hydroxyl groups involved in the synthesis of Ag NPs, which reduced silver and can no longer bind with water, as well as due to capillary forces. The decrease in absorption capacity should be attributed to a decrease in the number of BC pores due to the inclusion of Ag NPs, which leads to a decrease in water retention capacity.

It was found that in a solution of $AgNO_3$ of different concentrations (0.0001, 0.001 and 0.01 M) with a stabilization of the medium temperature at

60°C, the water retention capacity decreased with an increase in the content of Ag NPs (Figure 10). Thus, the BC / Ag NPs absorbed in the samples can be located between the fibers or inside the fibers, since it leads to the movement of Ag NPs through the fibrous structure. It can cause maceration of the surrounding skin during clinical use and helps support the wound healing process. Our result was confirmed by other researchers [24].

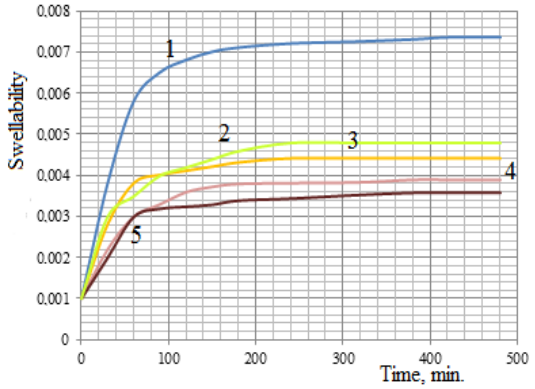

Figure 10. *Swelling capacity of a pure BC film and a composite BC / Ag NPs, 1 mol · L^{-1}. BC (1), BC/Ag NPs 60°C (2), BC/* $AgNO_3$ 0.0001M (3), BC/ $AgNO_3$ 0.001 M (4), BC/ $AgNO_3$ 0.01 M (5).

3.4. Wetting Angle

The surface energy is usually considered to be a quantity consisting of two components – the dispersion and polar, so according to the well-known Owens and Wendt equation [25], where the wetting edge angle is used, these components and, accordingly, the total surface energy were determined. BC is a hydrophilic material, the value of the edge angle of wetting with water is less than 50° (43.5). The surface energy of the composites of BC / Ag NPs determined the sorption wettability of low molecular weight substances. The surface (hydrophobicity and hydrophilicity) of the composites of BC / Ag NPs is an integral part of the structure; upon wetting, they change and contribute to the change in the surface energy and its components.

Compared with the original BC films, the composites with Ag NPs had a hydrophobic surface, an indirect indicator of which is an increase in the value of the contact angle of wetting with water (Table 2).

Changes in the values of contact angles are given at temperatures of 30℃, 60℃ and 90℃, respectively. For composites BC / Ag NPs, the contact angle of water wetting increased with an increase in the content of Ag NPs, with an increase in both dispersed and polar components.

Table 2. *Surface energy of composites of BC / Ag NPs.*

Samples	The edge angle of wetting with water θ, º	Disperse component σ^D, mJ / m^2	Polar component σ^P, mJ / m^2	Surface energy σ, mJ / m^2
BC	49	30	18	48
BC/ Ag NPs 0.001 M				
30℃	58	44	20	68
60℃	57	43	19	62
90℃	57	42	18	60
BC/ Ag NPs at 60℃				
0.0001 M	50	39	25	64
0.001 M	59	44	21	65
0.01 M	68	46	23	69

3.5. X-ray Diffraction Pattern of BC and BC / Ag NPs

According to three diffraction lines with interplanar spacings d = 6.0320 Å, 5.1869 Å, 3.88583 Å, this phase can be attributed to cellulose, there are Miller indices, respectively 100, 010 and 110 (Figure 11). The X-ray diffraction pattern contains two more diffraction lines, which are may be of a different type of cellulose. Therefore, Table 3 shows the interplanar distances of the lines of the analyzed phase and the sizes of crystallites in composites with different silver contents. Crystallinity refers to the degree of structural order in a solid; in a crystal, the arrangement of atoms or molecules is consistent and repetitive. According to a scheme on the Figure 2, Ag NPs are replaced instead of hydrogen atoms.

Table 3. *Results of processing diffraction patterns of BC and BC / Ag NPs.*

Samples	Miller indices, Å			FWHM	Crystallite size
	100	010	110		
BC	6.032	5.186	3.885	1.334	109
BC / Ag NPs 0.001 M					
30°C	6.153	5.312	3.935	1.382	118
60°C	6.079	5.239	3.904	1.337	122
90°C	6.011	5.219	3.891	1.342	121
BC / Ag NPs at 60°C					
0.0001 M	6.103	5.256	3.904	1.435	114
0.001 M	6.079	5.239	3.894	1.374	119
0.01 M	6.032	5.186	3.885	1.354	121

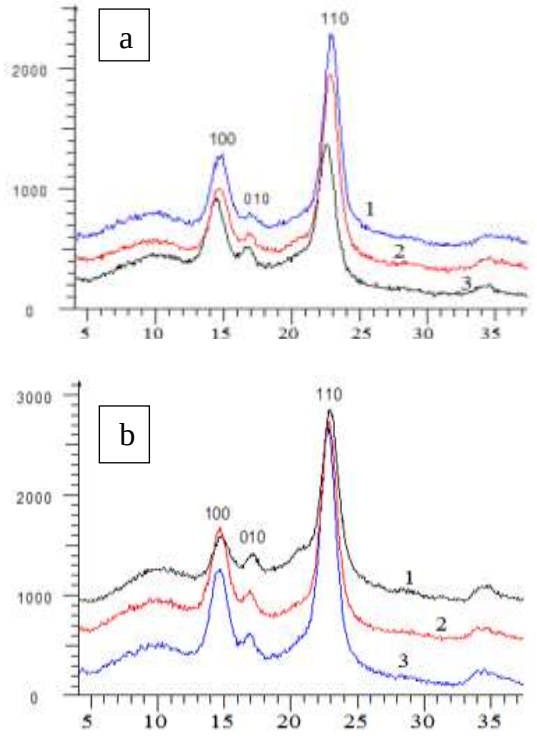

Figure 11. *X-ray diffraction patterns of the BC composite with Ag NPs obtained at different temperatures (a): BC/Ag NPs 90°C (1), BC/Ag NPs 60°C (2), BC/Ag NPs 30°C (3); and at different concentrations of $AgNO_3$ in the reaction solution (b): BC/ $AgNO_3$ 0.01 M (1), BC/ $AgNO_3$ 0.001 M (2), BC/ $AgNO_3$ 0.0001M (3).*

It can be seen from the data in Table 3 that with an increase in temperature, the parameters of the crystal lattice of cellulose decrease, and the sizes of crystallites do not depend on temperature. With a decrease in the silver content in the composites, the values of the interplanar distances of the lines increase, that is, the crystal lattice parameter of cellulose increases.

Also, with a decrease in the silver content in the samples, the crystallite sizes decrease.

3.6 Antimicrobial Susceptibility Test Results

It is known from the literature [26, 27] that Ag NPs with a size of 10 ~ 100 nm have a unique size and surface effect, which can penetrate the pathogen and easily integrate with-SH-bonds in the bacterial enzyme protein. Enzymes in bacteria can lose their activity due to the inclusion of silver, which leads to bacterial death, tissue repair, and accelerated wound healing.

Table 4. *Diameter of the zones of bacterial growth inhibition by composite BC films with Ag NPs.*

Name of the microbial culture	Diameter of zones (mm)						
	BC	BC/Ag NPs 0.001 M			BC/$AgNO_3$ at 60°C		
		30 °C	60 °C	90 °C	0.0001 M	0.001 M	0.01 M
Escherichia (E.) coli ATCC 25922	-	1.7 ±0.2	3.2 ±0.5	4±0.6	3.7 ±0.2	5.8 ±0.3	6.2 ±0.6
Pseudomonas (P.) aeruginosa ATCC 27853	-	1.1 ±0.1	2.1 ±0.4	2.5 ±0.2	2.7 ±0.3	3.2 ±0.4	3.5 ±0.3
Staphylococcus (S.) aureus ATCC 25923	-	4±0.5	7.6 ±0.2	8.7 ±0.5	3.8 ±0.7	4.8 ±0.3	7.3 ±0.5

In this study, three reference strains (two Gram-negative: *Escherichia (E.) coli, Pseudomonas (P.) aeruginosa*, and one gram-positive - *Staphylococcus (S.) aureus*) were taken to evaluate the

antimicrobial activity of BC composites with Ag NPs in relation to test microbial cultures (Table 4).

Antimicrobial properties were determined by the method of the inhibition zone by diameter, the larger the inhibition zone, the stronger the antimicrobial property.

It was found that the inhibition efficiency depends on the size of the inhibition zone, the larger the net area around the film, the higher the inhibition efficiency. Antimicrobial activity was not observed in three microorganisms in comparison with the initial BC as a control zone of inhibition. This indicates that BC does not have antimicrobial properties.

It was found that composites obtained at higher temperatures and concentrations of the $AgNO_3$ solution, the level of embedded silver in BC films, showed a more pronounced inhibitory effect on bacteria. These results indicated that BC films containing Ag NPs have good antimicrobial activity, both against *Escherichia (E.) coli* and *Staphylococcus (S.) aureus*. It is known from the literature that the activity of Ag NPs depends on their size and quantity in the composite. It is believed that the minimum inhibitory concentration of Ag NPs is in the range from 0.05 to 0.1 mg / ml [28].

4. CONCLUSIONS

The resulting composites of bacterial cellulose (BC) films with silver nanoparticles (Ag NPs) were studied in detail, including Scanning Electron Microscopy (SEM), X-ray phase analysis, and UV-Visible Spectroscopy. A significant change in the UV-visible absorption spectrum, water retention capacity, the value of the water wetting edge angle, and the surface energy of BC/Ag NPs slightly depend on the temperature in the system. An increase in the $AgNO_3$ concentration in the reaction solution was accompanied by an increase in the silver content in the composites, since the water-holding capacity decreased and showed that the BC/Ag NPs with a more hydrophobic surface than the original BC.

It was found that differences in the structure, physical and chemical properties and surface characteristics affected the degree of inhibition of the pathogenic microorganism. All the obtained composites have antimicrobial activity in relation to the tested *Staphylococcus (S.) aureus, Pseudomonas (P.) aeruginosa, Escherichia (E.) coli*.

CONFLICT OF INTEREST

The authors declare that they have no conflict of interest.

REFERENCES

1. Beekmann, U., Zahel, P., Karl, B., Schmölz, L., Börner, F., Gerstmeier, J., Werz, O., Lorkowski, S., Wiegand, C., Fischer, D., Kralisch, D., "Modified bacterial cellulose dressings to treat inflammatory wounds", *Nanomaterials*, 10 (2020) 2508.
2. Amorim, J. D. P., Souza, K. C., Duarte, C. R., Duarte, I. S., Ribeiro, F. A. S., Silva, G. S., Farias, P. M. A., Stingl, A., Costa, A. F. S., Vinhas, G. M., Sarubbo, L. A., "Plant and bacterial nanocellulose: production, properties and applications in medicine, food, cosmetics, electronics and engineering. A review", *Environ Chem Lett*, 18 (2020) 851–869.
3. Moon, R. J., Martini, A., Nairn, J., Simonsen, J., Youngblood, J., "Cellulose nanomaterials review: structure, properties and nanocomposites", *Chem. Soc. Rev.*, 40 (2011) 3941-3994.
4. Ambekar, R. S., Kandasubramanian, B., "Advancements in nanofibers for wound dressing: A review", *Eur. Polym. J.*, 117 (2019) 304-336.
5. Felgueiras, H. P., Teixeira, M. A., Tavares, T. D., Homem, N. C., Zille, A., Amorim, M.T.P., "Antimicrobial action and clotting time of thin, hydrated poly(vinyl alcohol)/cellulose acetate films functionalized with LL37 for prospective wound-healing applications", *J. Appl. Polym. Sci.*, 137 (2020) 48626.
6. Suarato, G., Bertorelli, R., Athanassiou, A. "Borrowing from nature: biopolymers and biocomposites as smart wound care materials", *Front. Bioeng. Biotechnol.*, 6 (2018), DOI:10.3389/fbioe.2018.00137.
7. Buruaga-Ramiro, C., Valenzuela, S. V., Valls, C., Roncero, M. B., Pastor, F.I. J., Díaz, P., Martinez, J., "Development of an antimicrobial bioactive paper made from bacterial cellulose", *Int. J. Biol. Macromol.*, 158 (2020) 587-594.

8. Zheng, L., Li, Sh., Luo, J., Wang, X., "Latest advances on bacterial cellulose-based antibacterial materials as wound dressings", *Front. Bioeng. Biotechnol.*, 8 (2020), DOI: 10.3389/fbioe.2020.593768.
9. Rakhimova, B. U., Kudaibergenov, K. K., Tulepov, M. I., Sassykova, L. R., Spanova, G. A., Mansurov, Z. A., Savitskaya, I. S., "Preparation and determination of the physical and chemical properties of the nano-gel film of bacterial cellulose", *Dig. J. Nanomater. Biostructures*, 16 (2021) 1587-1593.
10. Suryanto, H., Muhajir, M., Susilo, B. D., Pradana, Y. R. A., Wijaya, H. W., Ansari, A. S., Yanuhar, U. "Nanofibrillation of bacterial cellulose using high-pressure homogenization and its films characteristics", *J. Renew. Mater.*, 9 (2021) 1717-1728.
11. Pogorelova, N., Rogachev, E., Digel, I., Chernigova, S., Nardin, D. "Bacterial cellulose nanocomposites: morphology and mechanical properties", *Materials*, 13 (2020) 2849–2816.
12. Mirmohammadsadegh, N., Shakoori, M., Moghaddam, H.N., Farhadi, R., Shahverdi, A. R., Amin, M. "Wound healing and anti-inflammatory effects of bacterial cellulose coated with Pistacia atlantica fruit oil", *DARU J. Pharm Sci.*, (2021), DOI:10.1007/s40199-021-00405-9.
13. Tabaii, M. J., Emtiazi, G., "Transparent nontoxic antibacterial wound dressing based on silver nano particle/bacterial cellulose nano composite synthesized in the presence of tripolyphosphate", *J. drug del. sci. tech.*, 44 (2018) 244-253.
14. Sukhorukova, I. V., Sheveyko, A. N., Shvindina, N. V., Denisenko, E. A., Ignatov, S. G., Shtansky, D. V., "Approaches for controlled Ag^+ ion release: influence of surface topography, roughness, and bactericide content", *ACS Appl. Mater. Interfaces*, 9 (2017) 4259-4271.
15. Paseban, N., Ghadam, P., Purohosseini, P. S., "The fluorscence behavior and stability of AgNP synthesized by juglan regia green husk aqueou extract", *Int. J. Nanosci. Nanotechnol*, 15 (2019) 117-126.
16. John, T., Parmar, K. A., Kotval, Sh. C., Jadhav, J., "Synthesis, characterization, antibacterial and anticancer properties of silver nanoparticles synthesized from carica papaya peel extract", *Int. J. Nanosci. Nanotechnol*, 17 (2021) 23-32.
17. Mittal, D., Narang, K., Leekha, A., Kumar, K., Verma, A.R., "Elucidation of biological activity of silver based nanoparticles using plant constituents of syzygium cumini", *Int. J. Nanosci. Nanotechnol.*, 15 (2019) 189-198.
18. Wu, Ch. N., Fuh, Sh. Ch., Lin, Sh. P., Lin, Y. Y., Chen, H. Y., Liu, J. M., Cheng, K. Ch., "TEMPO-oxidized bacterial cellulose pellicle with silver nanoparticles for wound dressing", *Biomacromolecules*, 19 (2018) 544-554.
19. Pal, S., Nisi, R., Stoppa, M., Licciulli, A., "Silver-functionalized bacterial cellulose as antibacterial membrane for wound-healing applications", *ACS Omega*, 2 (2017) 3632-3639.
20. Sajjad, W., Khan, T., Ul-Islam, M., Khan, R., Hussain, Z., Khalid, A., Wahid, F., "Development of modified montmorillonite-bacterial cellulose nanocomposites as a novel substitute for burn skin and tissue regeneration", *Carbohydr. Polym.*, 206 (2019) 548-556.
21. Sarkandi, A. F., Montazer, M., Harifi, T., Rad, M. M., "Innovative preparation of bacterial cellulose/silver nanocomposite hydrogels: In situ green synthesis, characterization, and antibacterial properties", *J. Appl. Polym. Sci.*, 138 (2021) 49824.
22. Caschera, D., Toro, R. G., Federici, F., Montanari, R., Caro, T., Al-Shemy, M. T., Adel, A. M., "Green approach for the fabrication of silver-oxidized cellulose nanocomposite with antibacterial properties", *Cellulose*, 27 (2020) 8059-8073.
23. Elayaraja, S., Liu, G., Zagorsek, K., Mabrok, M., Ji, M., Ye, Zh., Zhu, S., Rodkhum, Ch., "TEMPO-oxidized biodegradable bacterial cellulose (BBC) membrane coated with biologically-synthesized silver nanoparticles (AgNPs) as a potential antimicrobial agent in aquaculture (In vitro)", *Aquaculture*, 530 (2021) 735746.
24. Spagnol, C., Fragal, E. H., Pereira, A. G.B., Nakamura, C. V., Muniz, E. C., Follmann, H. D. M., Silva, R., Rubira, A. F., "Cellulose nanowhiskers decorated with silver nanoparticles as an additive to antibacterial polymers membranes fabricated by electrospinning", *J. Colloid Interface Sci.*, 531 (2018) 705-715.
25. Lee, K. M., Ngo, Ch. V., Jeong, J. Y., Jeon, E., J. Je, T., Chun, D. M., "Fabrication of an anisotropic superhydrophobic polymer surface using compression molding and dip coating", *Coatings*, 7 (2017) 194.
26. Khatoon, U. T., Nageswara Rao, G. V. S., Mohan, M. K., Ramanaviciene, A., Ramanavicius, A., "Comparative study of antifungal activity of silver and gold nanoparticles synthesized by facile chemical approach", *J. Environ. Chem. Eng.*, 6 (2018) 5837-5844.
27. Garza-Cervantes, J.A., Mendiola-Garza, G., de Melo, E.M., Dugmore, T. I. J., Matharu, A.S., Morones-Ramirez, J.R., "Antimicrobial activity of a silver-microfibrillated cellulose biocomposite against susceptible and resistant bacteria", *Sci. Rep.*, 10 (2020), 7281, DOI:10.1038/s41598-020-64127-9.
28. Mousavi, S. M., Hashemi, S. A., Ghasemi, Y., Atapour, A., Amani, A.M., Dashtaki, A. S., Babapoor, A., Arjmand, O., "Green synthesis of silver nanoparticles toward bio and medical applications: review study", *Artif Cells Nanomed Biotechnol.*, 46 (2018) S855-S872.